Comparative studies of MCMB and C–C composite as anodes for lithium-ion battery systems

Sohrab Hossain[*], Yong-Kyu Kim, Yousry Saleh, Raouf Loutfy

LiTech, LLC, 7960 S. Kolb Road, Tucson, AZ 85706, USA

Abstract

Mesocarbon microbead (MCMB 2528) and C–C composite have been investigated as anodes for lithium-ion batteries using half-cells with lithium counter electrode and three electrode cell systems containing $LiCoO_2$ cathode and lithium reference electrodes in 1 M $LiPF_6$ electrolyte (EC/DMC 1:1 v/v). The test results show that the practical capacity of C–C composite anode is 50% higher than that of MCMB-based anode (based on total anode weight). The irreversible capacity loss of C–C composite is significantly lower than that of MCMB carbon. Lithium-ion cells made with C–C composite anode can accept repeated overdischarge without performance deterioration. The extra capacity of C–C composite can be utilized to improve energy density and safety issues related to overcharge of lithium-ion cells. Differential scanning calorimetry (DSC) results indicates that the thermal stability of fully charged C–C composite anode (lithiated anode) is much better than that of fully charged MCMB anode.
© 2002 Elsevier Science B.V. All rights reserved.

1. Introduction

Mesocarbon microbead (MCMB), artificial and natural graphite and carbon fiber are used as anodes for commercial lithium-ion batteries. Poly(vinyledene) fluoride (PVDF) is used as a binder to improve the mechanical integrity of the electrode. Copper is universally used as the substrate for the anode. Carbon or graphite material is mixed with PVDF in an organic solvent (*N*-methyl pyrolidinone, NMP or dimethyl formamide, DMF) and the mixture is coated onto the copper substrate to produce the anode. The present carbon or graphite anode contains only 65% or less of active material.

Sato et al. [1] disclosed a carbonaceous material prepared by heating polyparaphenylene at 700 °C which has a reversible capacity of 680 mAh/g. Several other researchers [2,3] confirmed this finding. At the same year, Mabuchi et al. [4] disclosed a low density (about 1.5 g/cc) carbonaceous material prepared by heating coal tar pitch at 700 °C which has a reversible capacity of about 750 mAh/g. These values are much greater than that of the carbon, graphite, or carbon fiber used in lithium-ion batteries. But due to high irreversible

capacity loss and a significantly lower-density, these carbonaceous materials have not been used in commercial lithium-ion batteries.

Recently, carbon–carbon (C–C) composite has been proposed as a potential candidate as an anode for lithium-ion battery systems [5]. C–C composite, on the other hand, does not contain any inactive material (no binder or metal substrate) and the entire composite electrode provides active sites for lithium-ion intercalation and, therefore, can be considered as a high capacity anode for lithium-ion batteries. However, due to the absence of a metallic substrate, C–C composite anode may not be able to provide comparable rate capabilities of carbon or graphite anode with copper substrate. It is, therefore, of interest to examine and compare the rate capability of C–C composite and MCMB anodes.

The carbon, graphite, carbon fiber or C–C composite materials can deliver a specific capacity of 372 mAh/g and capacity density of 820 mAh/cc corresponding to the chemical formula LiC_6 as compared to 3862 mAh/g and 2047 mAh/cc of metallic lithium. However, the predicted practical specific capacity (mAh/g) and capacity density (mAh/cc) of carbon, graphite, carbon fiber or metallic lithium are significantly lower than those mentioned above and the predicted values for C–C composite are found to be comparable to that of metallic lithium as shown in Table 1.

---

[*] Corresponding author. Tel.: +1-520-574-1980x23.
E-mail address: shossain@mercorp.com (S. Hossain).

Table 1
Comparison of predicted usable capacity of lithium, carbon, and C–C anode

| Characteristics	Li metal	Lithiated carbon or graphite	Lithiated C–C composite
Theoretical specific capacity (Ah/kg)	3862	372	372
Theoretical capacity density (Ah/l)	2047	820	820
Apparent specific capacity (Ah/kg)			
Four-fold excess of lithium	966		
95% active material in carbon electrode		353	
100% active material in C–C composite electrode			372
Apparent capacity density (Ah/l)			
Four-fold excess of lithium	512		
30% porosity of carbon electrode		574	
30% porosity of C–C composite electrode			574
Practical usable specific capacity (Ah/kg)			
Substrate weight is two times of lithium weight	322		
Substrate weight is 1/2 of active carbon weight		235	
10% of C–C composite electrode unused			335
Practical usable capacity density (Ah/l)			
10 μm thick substrate for lithium electrode	450		
10 μm thick substrate for carbon electrode		535	
10% of C–C composite electrode unused			517
Summary			
Practical usable specific capacity (Ah/kg)	322	235	335
Practical usable capacity density (Ah/l)	450	535	517

This communication compares the performance characteristics of MCMB 2528 carbon and C–C composite as anodes for lithium-ion battery systems.

2. Experimental

The details fabrication procedures of lithium, C–C composite, and LiCoO$_2$ electrodes were described elsewhere [5]. MCMB carbon electrode was prepared from a slurry of 95% MCMB 2528 and 5% poly(vinyledene fluoride) in dimethyl formamide. The slurry was coated onto 10 μm thick copper substrate. The coated substrate was dried over hot air, pressed, and then cut to the size of other electrodes. The dimension of all electrodes for half-cells was 2.5 cm × 3.5 cm. The dimension of working and counter electrodes was 1.5 cm × 3.0 cm and that of reference electrode was 1.5 cm × 1.5 cm for the three electrode lithium-ion cells.

The C–C composite was made from a pitch-based carbon fiber and heat-treated to 2850 °C. The thickness of the composite was 110 μm and that of MCMB electrode was
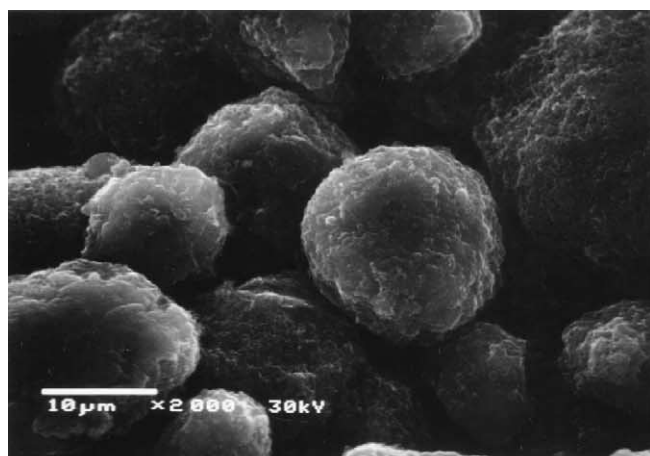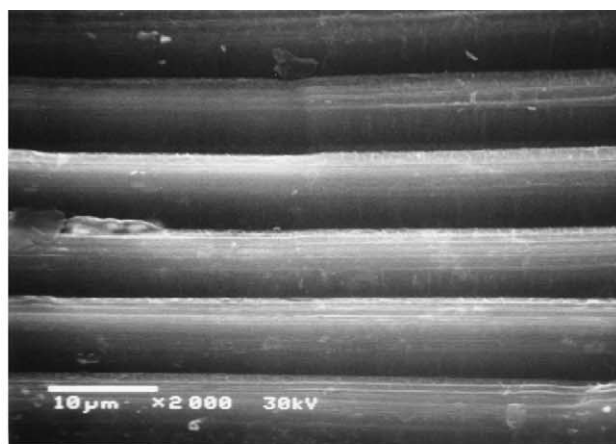
Fig. 1. SEM images of the in-plane views of (a) MCMB and (b) C–C composite electrode.
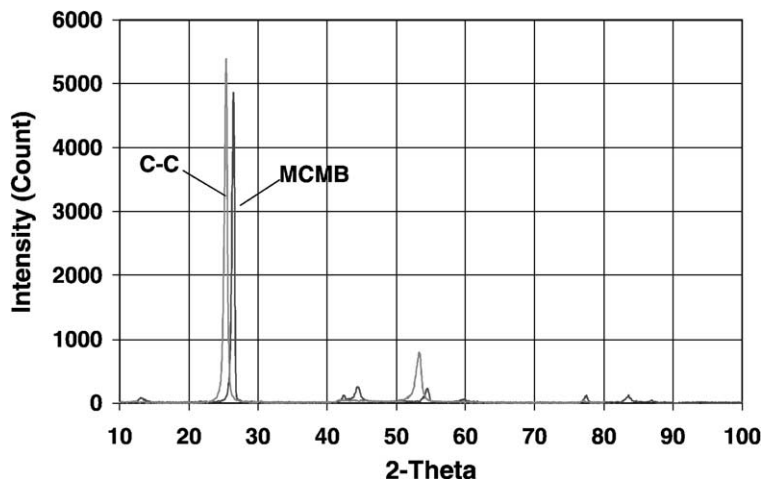
Fig. 2. X-ray diffraction patterns of MCMB and of C–C composite.

120 μm (110 μm without substrate). The density of both C–C composite and MCMB electrodes was 1.5 g/cc. The in-plane views of MCMB and C–C composite electrodes are shown in Fig. 1(a) and (b), respectively. C–C composite is composed of carbon fibers. The shape of MCMB carbon is spherical. Fig. 2 shows a comparison of the X-ray diffraction patterns of the C–C composite with MCMB carbon. The $d_{0\,0\,2}$ spacing of the C–C composite and MCMB are 0.349 and 0.337 nm, respectively. The higher interlayer spacing of the composite electrode allows lower expansion during lithium-ion intercalation.

The development of half-cells with C–C composite or MCMB carbon working electrodes and metallic lithium counter electrodes is similar to that described in [5]. The schematic diagram of three electrode systems containing C–C composite or MCMB working electrode, $LiCoO_2$
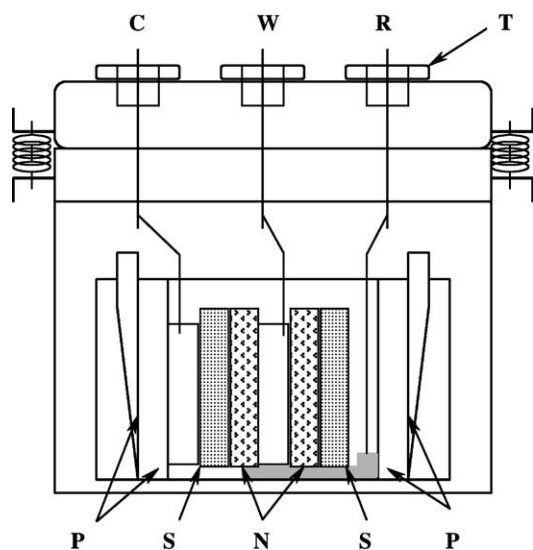

Fig. 3. Schematic diagram of three electrode cell. C: counter electrode, W: working electrode, R: reference electrode, S: separator, N: non-woven cloth, P: polypropylene washer, T: Teflon cap.

counter electrode, and metallic lithium reference electrode is shown in Fig. 3.

The electrochemical measurements of the half-cells and three electrode cells were carried out using an Arbin Model BT 2043 (ABTS 4.0) cycler. The half-cells were first discharged at a constant current to 0.00 V, allowed to rest at open-circuit voltages (OCV) for 5 min, and then charged at the same rate to a cut-off voltage of 1.00 V. The half-cells were discharged and charged under the above voltage regime for several times until a fairly constant values of charge capacities were obtained. This reversible charge capacity was considered as the capacity of the working electrode. The cells were then used for the evaluation of rate capability.

The three electrode cells were first charged at a constant current to 4.2 V and then discharged at the same rate to a cut-off voltage of 2.5 V for C–C composite-based cells and 2.75 V for MCMB-based cells. The variations of anode and cathode voltages with respect to lithium during the charge discharge process were also measured.

3. Results and discussion

A number of half-cells were made with C–C composite or MCMB carbon working electrodes and metallic lithium counter electrode to measure the irreversible capacity loss, apparent and true specific capacity (mAh/g) and capacity density (mAh/cc), and rate capability of the C–C composite and MCMB carbon materials. Charge–discharge profiles of lithium-ion cells made with MCMB carbon and C–C composite electrodes are also analyzed with respect to lithium reference electrode.

3.1. Irreversible capacity loss

Several half-cells were made with MCMB and C–C composite working electrode and metallic lithium counter electrode in 1 M $LiPF_6$ electrolyte (EC/DMC 1:1). The
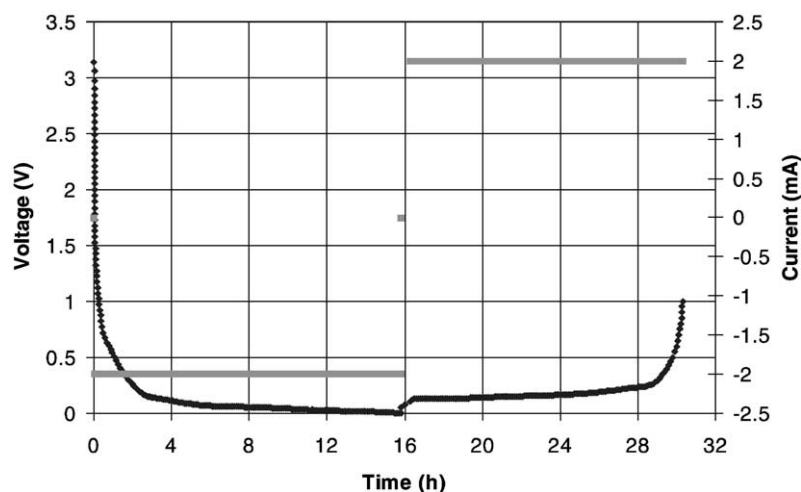
Fig. 4. First discharge charge behavior of MCMB carbon in 1 M LiPF$_6$ electrolyte. Counter electrode: Li.

open-circuit voltages of these cells were in the range of 3.13–3.15 V. Figs. 4 and 5 represent the first discharge (intercalation of lithium-ions) and charge (de-intercalation of lithium-ions) profiles of the half-cells made with MCMB 2528 carbon (LMB001) and C–C composite (CCL016) working electrodes, respectively. The cells were discharged at a constant current of 2 mA to 0.00 V and then charged at the same rate of 2 mA to a cut-off voltage of 1.00 V. The first discharge capacity of the MCMB- and C–C composite-based cells was 31.8 and 30.0 mAh and the corresponding charge capacity was 28.9 and 29.1 mAh, respectively. The irreversible capacity losses of MCMB carbon and C–C composite were, therefore, 9 and 3%, respectively. The low irreversible capacity loss of C–C composite is most probably related to the low surface area (∼0.2 m^2/g), absence of binder and foreign materials and little or no surface functional groups present in the C–C composite [5,6].

Fig. 6 shows a part of the first discharge profiles of two MCMB (LMB001 and LMB002)- and two C–C composite (CCL016 and CCL017)-based half-cells. All these cells were discharged at 2 mA current drain. It is clearly evident that at higher voltage of the discharge profile, MCMB carbon contributes more capacity than C–C composite. For example, when discharged to 0.4 V, MCMB carbon contributed 2.75 mAh capacity as compared to only 0.84 mAh capacity obtained from C–C composite. The most of the irreversible capacity loss is associated with the capacity obtained at higher voltage of the first discharge where electrolyte reacts with foreign materials and active surface functional groups and are also used up to form a protective solid electrolyte interface (SEI) layer. Once these undesired reactions are complete and the protective layer is fully formed, there should not have any more irreversible capacity loss.
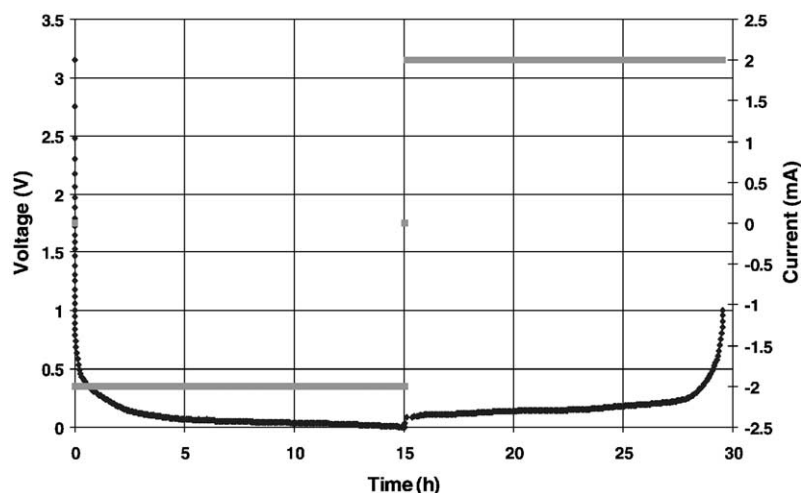

Fig. 5. First discharge charge behavior of C–C composite in 1 M LiPF$_6$ electrolyte. Counter electrode: Li.
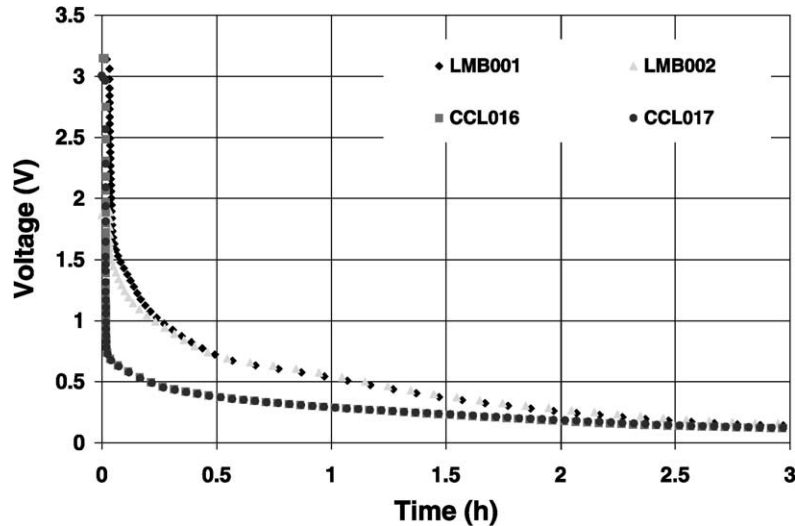
Fig. 6. First discharge behavior of MCMB and C–C composite in 1 M LiPF$_6$ electrolyte. Counter electrode: Li.

We continued cycling the MCMB (LMB001 and LMB002) and C–C composite (CCL016 and CCL017) cells. All these cells showed little or no irreversible capacity loss in the subsequent cycles. Fig. 7 shows a part of the second cycle discharge profiles of the two MCMB and the two C–C composite half-cells. The discharge profiles of MCMB and C–C composite-based half-cells, unlike first cycle, now almost overlap with each other.

3.2. Apparent specific capacity and capacity density

An experimental comparison of apparent specific capacity (mAh/g) and apparent capacity density (mAh/cc) of MCMB and C–C composite materials for the de-intercalation of lithium-ions are shown in Figs. 8 and 9, respectively. The charge profiles shown in the plots are for the cells LMB001 and CCL016. The values are calculated based on the amount

of carbon materials only and the contributions of inactive components such as copper substrate and PVDF binder for MCMB electrodes are ignored. The density of both MCMB and C–C composite electrodes was the same, 1.5 g/cc. The observed specific capacity and capacity density of MCMB are 341 mAh/g and 512 mAh/cc and for C–C composite, the values are 322 mAh/g and 484 mAh/cc, respectively. The observed apparent values of MCMB are slightly higher than that of C–C composite material.

3.3. True specific capacity and capacity density

Carbon–carbon composite electrode contains no binder and it does not have any metallic substrate. The entire C–C composite electrode is active for lithium-ion intercalation and, therefore, there is no difference between the apparent and true specific capacity and capacity density values for
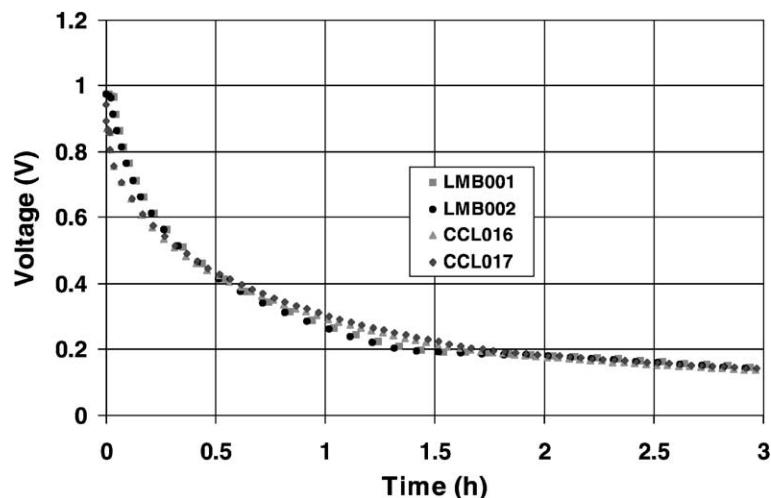

Fig. 7. Initial discharge behavior of MCMB and C–C composite after completion of first cycle. Electrolyte: 1 M LiPF$_6$; counter electrode: Li.
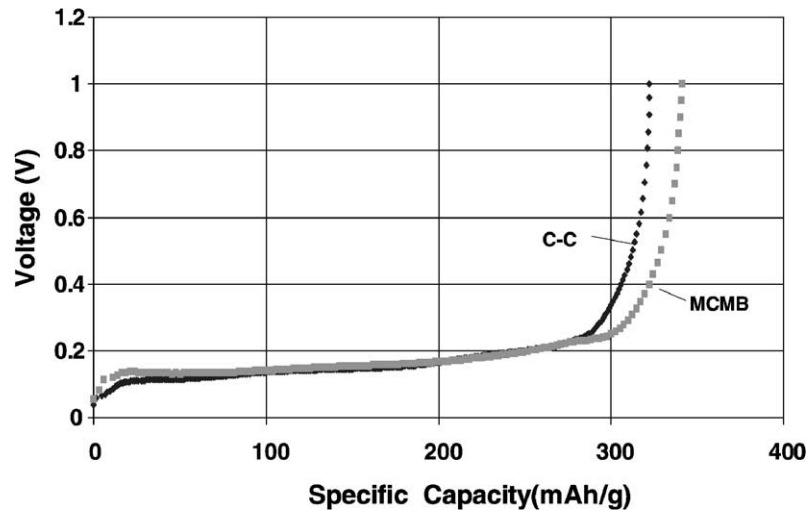
Fig. 8. Comparison of apparent specific capacity of C–C composite to MCMB carbon in 1 M LiPF$_6$ electrolyte at 0.5 mA/cm^2.

C–C composite electrodes. On the other hand, electrodes made with disordered hard carbon or graphite powder must contain binder to improve the mechanical integrity and adhesive characteristics and need an electronically conductive substrate as current collector. Because of excellent electrochemical stability within the operating voltage limit, copper is universally used as substrate for carbon anode. The substrate and binder are inactive; but their weight and volume make significant differences in true usable specific capacity and capacity density.

Figs. 10 and 11 compare the true usable specific capacity and capacity density of MCMB and C–C composite electrodes, respectively. The true specific capacity and capacity density of MCMB electrodes were calculated based on a copper substrate of 10 μm thick which is coated on both sides and the MCMB electrodes contain 5% PVDF binder. The true usable specific capacity of MCMB-based electrode is only 2/3 of that of C–C composite-based electrode. The C–C composite electrode can, therefore, be used as anodes

for the development of high specific energy and energy density lithium-ion cells. The true capacity density (mAh/cc), however, of the MCMB and C–C composite electrodes are comparable.

3.4. Safety and specific energy

C–C composite anode offers approximately 30–35% excess specific capacity compared to MCMB based anode as shown in Table 2. This excess capacity can be utilized to improve the specific energy and/or to address the safety issues of lithium-ion cells.

The present carbon anode of commercial lithium-ion cells, when fully charged, become golden yellow color LiC$_6$. LiC$_6$ is highly reactive. If C–C composite was used as anode and left 30–35% capacity unused, after fully charged, the C–C composite anode would become LiC$_x$, where x is much higher than 6. LiC$_x$ would then be less reactive than LiC$_6$.
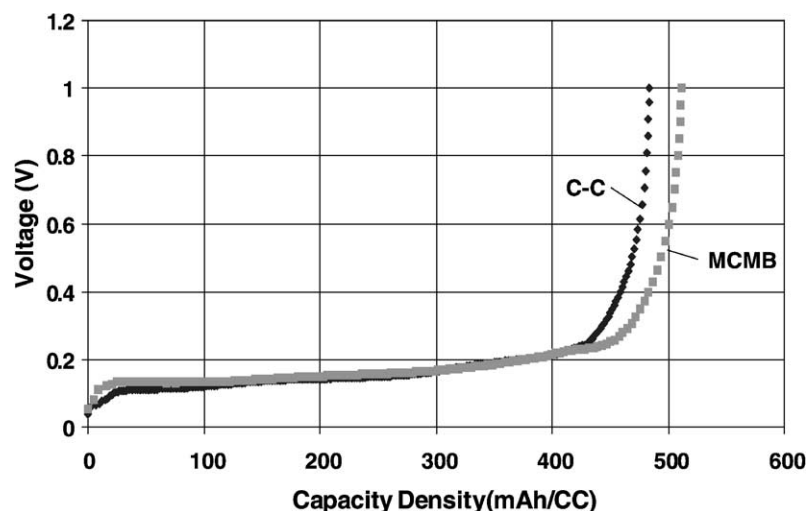

Fig. 9. Comparison of apparent capacity density of C–C composite to MCMB carbon in 1 M LiPF$_6$ electrolyte at 0.5 mA/cm^2.
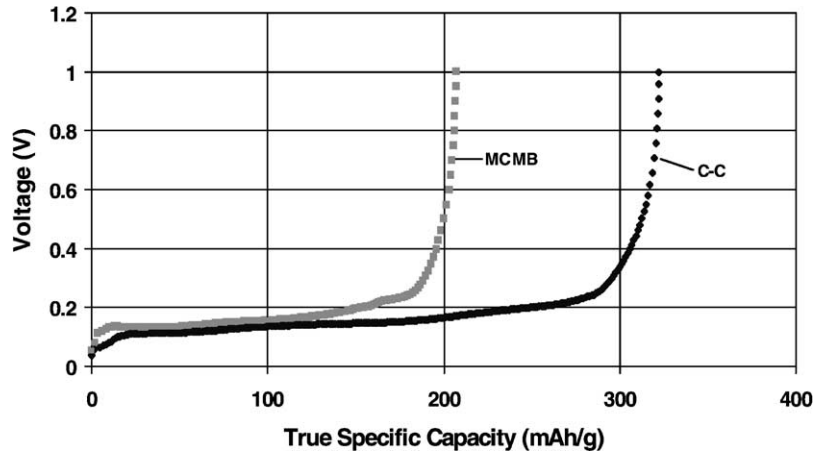
Fig. 10. Comparison of true specific capacity of C–C composite to MCMB carbon.

During overcharge of C–C composite-based lithium-ion cells having 30–35% excess anode capacity, lithium-ions transfer from cathode to anode and intercalate to form LiC_{x+y} until solvent decomposition dominate at cathode. There is, therefore, no metallic lithium deposition at the anode and thus can avoid thermal runaway of the lithium-ion cells. C–C composite-based lithium-ion cells, therefore, can offer inherently safe cell chemistry.

3.5. Rate capability

The rate capability of C–C composite and MCMB carbon has been investigated in 1 M $LiPF_6$ electrolyte in EC/DMC (1/1 v/v). The mass of C–C composite electrode was 0.118 g and the active mass of MCMB electrode was 0.124 g. The composition of MCMB electrode was 95% MCMB and 5% PVDF. The dimension of both the electrodes was $2.5\,cm \times 3.5\,cm$. The electrode loading was, therefore, 6.7 mg/cm^2 for C–C composite electrode and 7.1 mg/cm^2 for MCMB electrode.

Figs. 12 and 13 show the charge (de-intercalation of lithium-ions) characteristics of C–C composite and MCMB carbon, respectively, at different rates. At 2C rate, the C–C electrode was able to deliver 90% of its C/3 rate capacity. Similar rate capability was observed for MCMB electrode. The high rate capability of C–C composite is probably related to the fact that in C–C composite lithium-ion

Table 2
Comparison of capacity of C–C composite and MCMB anode

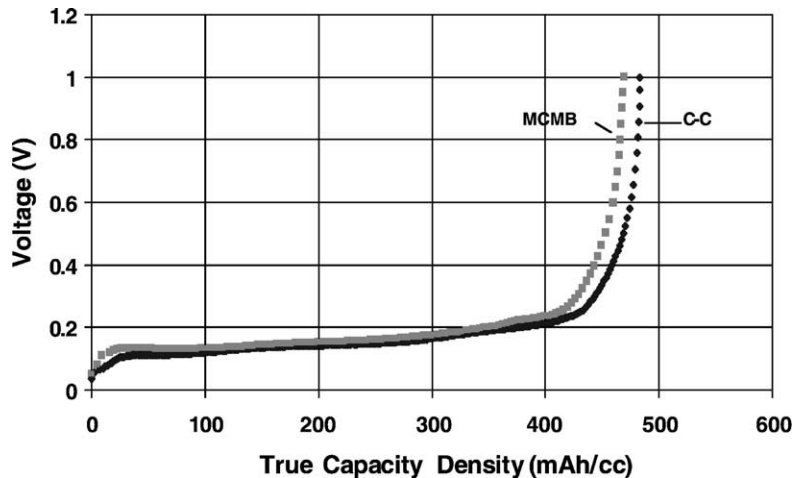| Anode material	Specific capacity of material (mAh/g)	Unused material	Anode specific capacity (mAh/g)	Anode capacity density (mAh/cc)
C–C	320	0.0	320	448
C–C	320	0.1	288	403
C–C	320	0.2	256	358
C–C	320	0.3	224	314
C–C	320	0.35	208	291
C–C	320	0.4	192	269
MCMB	340	0.0	210	294

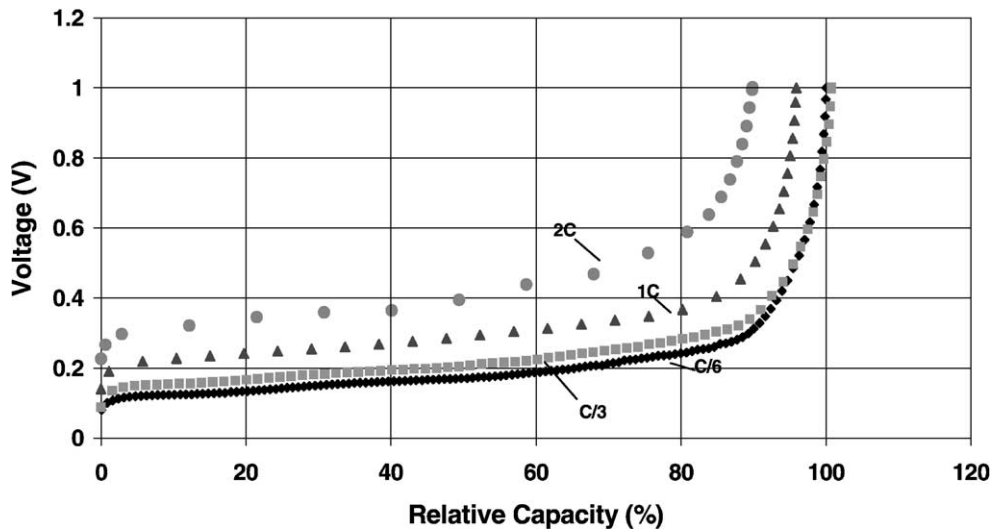Fig. 11. Comparison of true capacity density of C–C composite to MCMB carbon.

Fig. 12. Relative capacity of C–C composite at different rates. Counter electrode: Li; electrolyte: 1 M LiPF$_6$ in EC/DMC.

intercalation might have occurred at the surface of carbon fiber which is relatively facile than the intercalation of lithium-ions in carbon or graphite which occurs in between their interlayer spacing. The absence of binder might also have some positive effect on the rate for C–C composite electrode.

3.6. Study of lithium-ion cells with lithium reference electrode

In order to compare the behavior of individual electrode in lithium-ion cells during charge–discharge, overcharge, and overdischarge, several laboratory cells were made with C–C composite or MCMB anode, LiCoO$_2$ cathode, and lithium reference electrodes in 1 M LiPF$_6$ electrolyte (EC/DMC 1:1

v/v). The schematic diagram of the laboratory cell is shown in Fig. 3.

3.6.1. Charge discharge

The dimension and active material present in each electrode of the laboratory cells are given in Table 3. The practical capacity of LiCoO$_2$ cathode is significantly lower than that of MCMB or C–C composite anode.

The cells were first charged at 1 mA to 4.2 V and then discharged at the same rate to a cut-off voltage of 2.75 V for the MCMB and 2.5 V for the C–C composite cells. The very first charge discharge voltage profiles of the anode, cathode, and full cell made with the MCMB and C–C composite anodes with respect to lithium reference electrode and their comparisons are shown in Fig. 14. The voltage axes for
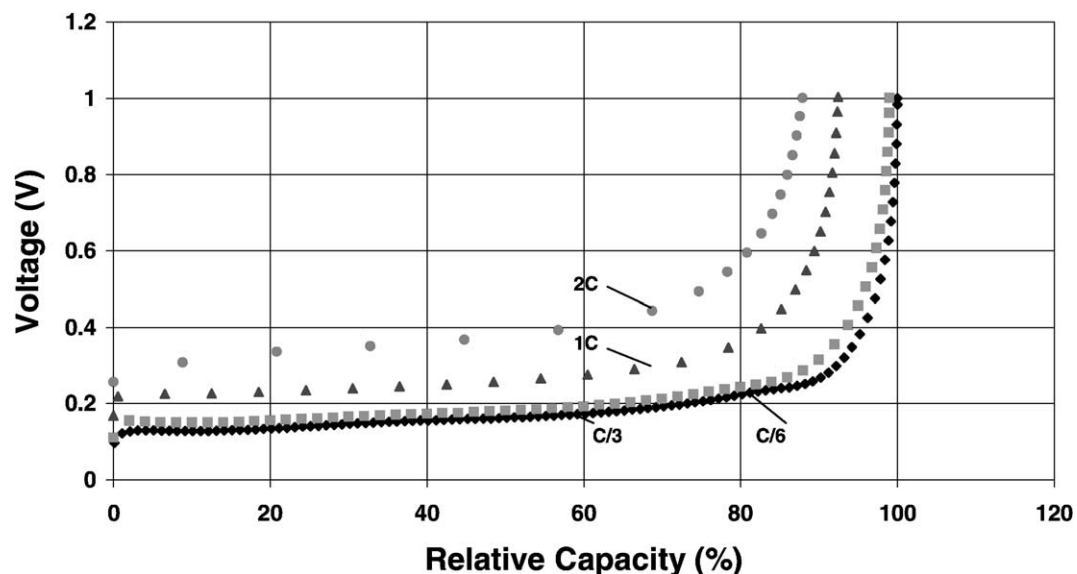

Fig. 13. Relative capacity of MCMB 2528 carbon at different rates. Counter electrode: Li; electrolyte: 1 M LiPF$_6$ in EC/DMC.

Electrode	Dimension without substrate (mm³)	Amount of active material (mg)
MCMB	$15 \times 30 \times 0.11$	64.7
C–C composite	$15 \times 30 \times 0.10$	67.5
LiCoO₂	$15 \times 30 \times 0.08$	100.1
Lithium	$15 \times 15 \times 0.05$	47.1

MCMB and C–C composite cells are shifted for clarity. Careful observation of the voltage profiles reveals that C–C composite anode is less polarized than MCMB anode during discharge. However, the effect is significantly low and may not be considered as an advantage of C–C composite.

The first charge capacities for the MCMB and C–C composite-based cells were 13.4 and 12.7 mAh, and the corresponding discharge capacities were 10.7 and 10.8 mAh,

respectively. The charge discharge capacity values for the MCMB and C–C composite cells are almost the same.

3.6.2. Overcharge

The variation of individual electrode and cell voltages during overcharge has also been investigated using cells having (i) practical capacity of anode equals to the practical capacity of cathode and (ii) the practical capacity of anode equals to 30–35% higher than the practical capacity of cathode and are discussed in the following sections.

3.6.2.1. Case I: practical capacity of anode equals practical capacity of cathode. Lithium-ion cells were made with LiCoO₂ cathode and MCMB (3CMB) or C–C composite (3CCC) anode with metallic lithium reference electrode in flooded electrolyte (1 M LiPF₆). The dimension of the cathode and anode was 1.5 cm × 3.0 cm. For MCMB cell (3CMB), the active mass of the anode was 69 mg, which
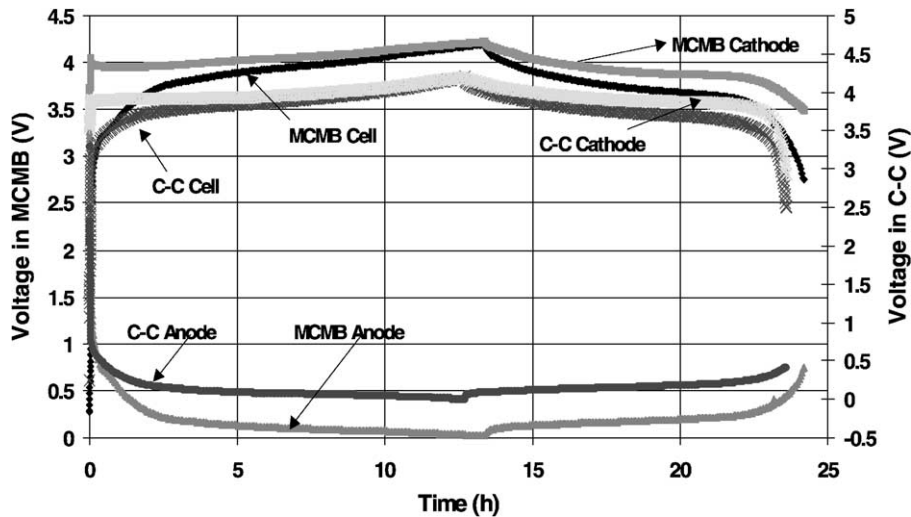

Fig. 14. Variation of anode, cathode, and cell voltages of MCMB and C–C composite-based lithium-ion cells with respect to lithium reference electrode. Cathode: LiCoO₂.
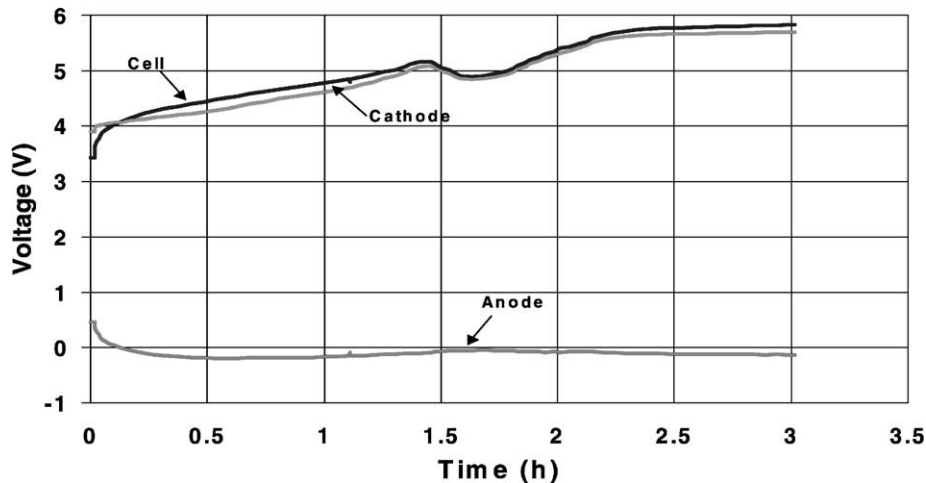

Fig. 15. Variation of anode, cathode, and cell voltages during overcharge of a MCMB based lithium-ion cell. Cathode: LiCoO₂; reference: Li.
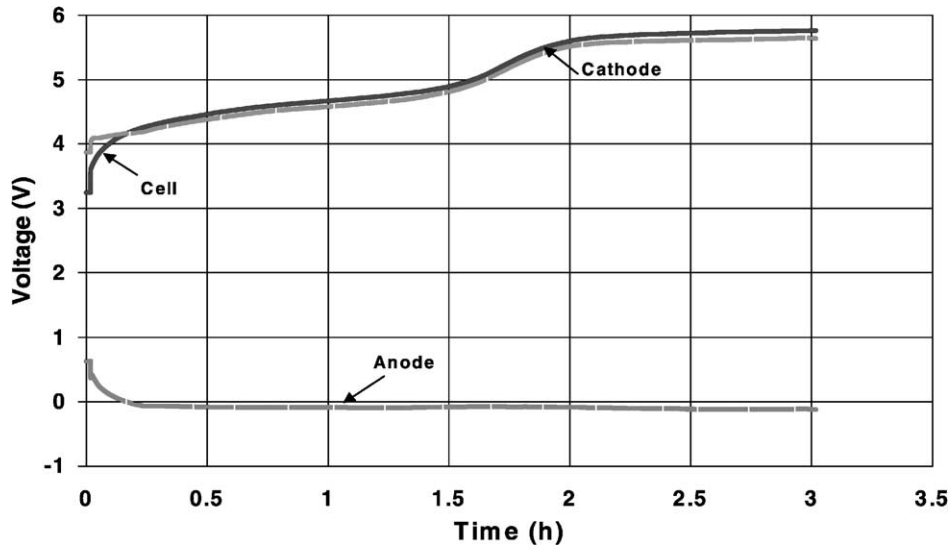
Fig. 16. Variation of anode, cathode, and cell voltages during overcharge of a C–C composite-based lithium-ion cell. Cathode: LiCoO$_2$; reference: Li.

corresponds to the practical capacity of 23 mAh (based on 340 mAh/g) and the active mass of cathode was 157 mg, the practical capacity of which is 22 mAh (assuming practical capacity of LiCoO$_2$ is 140 mAh/g). For C–C composite-based cell, the anode mass was 67 mg, which provides a practical capacity of 22 mAh (based on 322 mAh/g) and the active mass of cathode was 159 mg (practical capacity of 22 mAh).

Figs. 15 and 16 compare the individual electrode and cell voltages of MCMB and C–C composite-based cells, respectively, during charge/overcharge. The charge/overcharge was carried out at 20 mA current rate. The maximum cell voltage during overcharge for MCMB cell was 5.83 V and for C–C cell was 5.76 V and the corresponding anode voltages were −127 and −120 mV, respectively. After 5 min of rest period,

the cell voltage dropped to 4.44 V for MCMB cell and 4.46 V for C–C composite cell and the corresponding anode voltages were −14 and +5 mV, respectively.

Both the overcharged cells were then transferred to the glove box, and took apart to examine if any metallic lithium deposited on the anodes. MCMB anode was black and a significant portion of the anode was covered with white metallic lithium. C–C composite anode was totally golden yellow in color and we also noticed a stripe of white metallic lithium deposition on the anode.

The results clearly indicate that metallic lithium deposition occurs during overcharge when the practical anode capacity is equal to the reversible cathode capacity. The C–C composite anode is golden yellow color whereas the MCMB anode is black after charged and overcharged at 1C
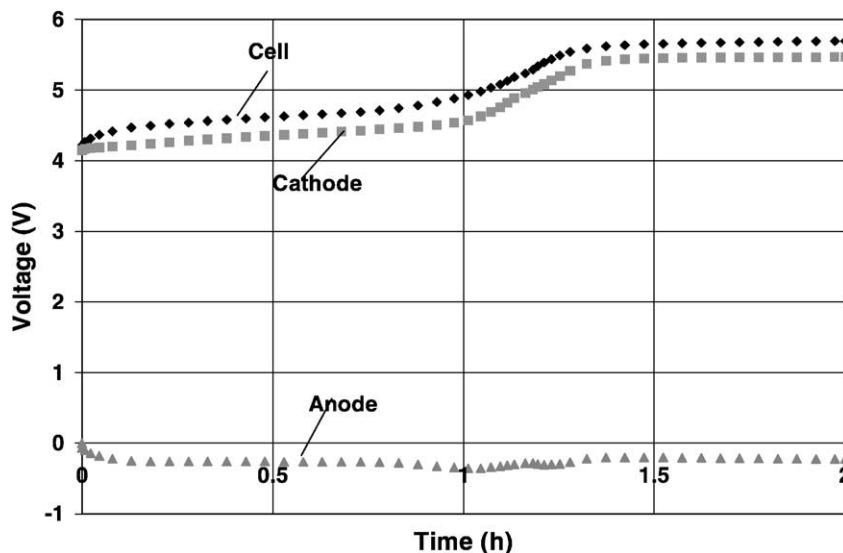

Fig. 17. Variation of anode, cathode, and cell voltages during overcharge of a MCMB based lithium-ion cell. Cathode: LiCoO$_2$; reference: Li.
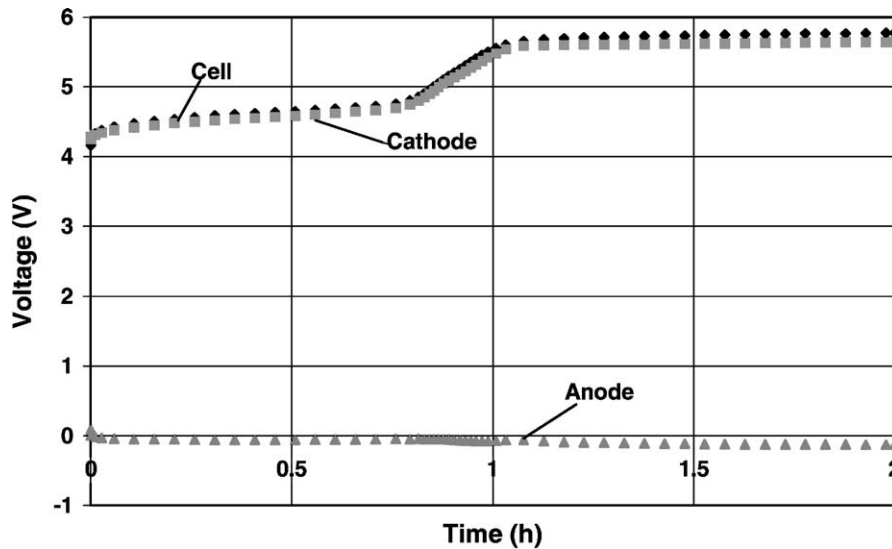
Fig. 18. Variation of anode, cathode, and cell voltages during overcharge of a C–C composite-based lithium-ion cell. Cathode: LiCoO$_2$; reference: Li.

rate indicating that the lithium-ion intercalation is more facile with C–C composite than with MCMB carbon.

3.6.2.2. Case II: practical capacity of anode 30–35% higher than that of cathode. Two lithium-ion cells were made with LiCoO$_2$ cathode and MCMB (3CMB) or C–C composite (3CCC) anode with metallic lithium reference electrode in flooded electrolyte (1 M LiPF$_6$). For MCMB-based cell (3CMB), the active mass of the anode was 58 mg, which corresponds to the practical capacity of 20 mAh (based on 340 mAh/g) and the active mass of cathode was 110 mg, the practical capacity of which is 15 mAh. For C–C composite-based cell, the anode mass was 61 mg, which provides a practical capacity of 20 mAh (based on 322 mAh/g) and the active mass of cathode was 110 mg.

Both the cells were first charged at 1.5 mA to 4.2 V prior to overcharge. Figs. 17 and 18 compare the individual

electrode and cell voltages of MCMB and C–C composite-based cells, respectively, during overcharge at 1C rate. The maximum cell voltage during overcharge for MCMB cell was 5.70 V and for C–C cell was 5.77 V and the corresponding anode voltages were −227 and −131 mV, respectively. During the rest period of 5 min (not shown in the figures), the cell voltage dropped to 5.0 V for MCMB cell and 5.1 V for C–C composite cell.

Both the overcharged cells were then transferred to the glove box and took apart to examine if any metallic lithium deposition occurred on the anodes. Both the MCMB and C–C composite anodes were golden yellow color and we did not notice any white metallic lithium deposition on the anodes at 1C rate of overcharge.

The results clearly indicate that the safety issues related to overcharge could be addressed by increasing the anode loading so that the anode can accept the extra capacity from
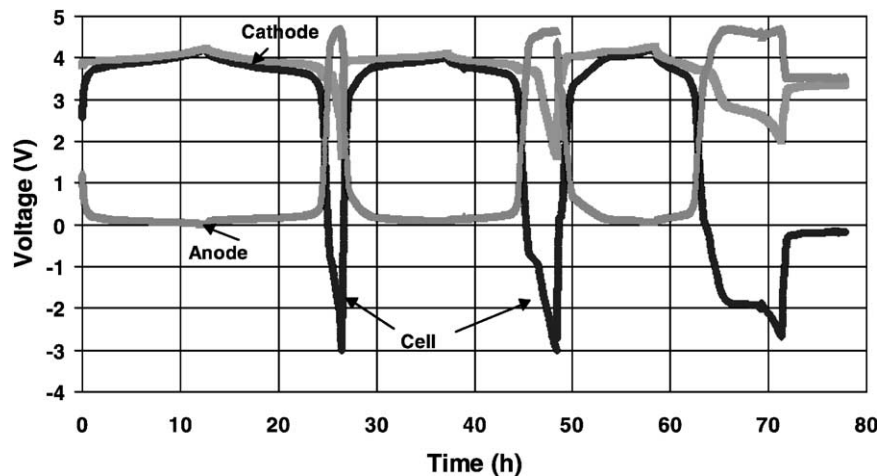

Fig. 19. Variation of anode, cathode, and cell voltages during charge, rest, and overdischarge of a MCMB anode based lithium-ion cell. Cathode: LiCoO$_2$; reference: Li.
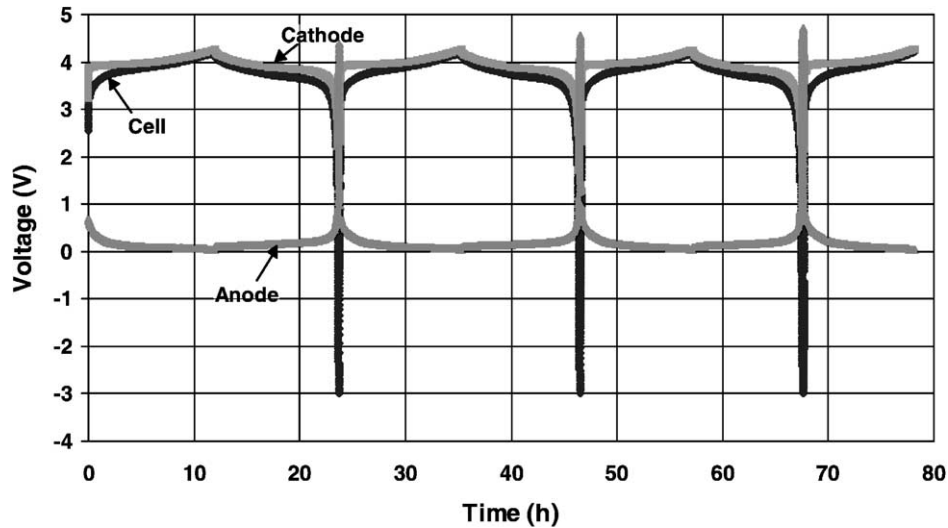
Fig. 20. Variation of anode, cathode, and cell voltages during charge, rest, and overdischarge of a C–C composite-based lithium-ion cell. Cathode: LiCoO$_2$; reference: Li.

the cathode during overcharge without metallic lithium deposition. For MCMB anode, however, the increase in loading results in thicker anode and, therefore, affects the cycle life and rate capability of the resulting lithium-ion cell [7]. C–C composite anode, which replaces metallic substrate with extra C–C composite, is therefore, particularly suitable to address the safety related overcharge problem.

3.6.3. Overdischarge

The overdischarge behavior of lithium-ion cells made with MCMB and C–C composite anodes and LiCoO$_2$ cathodes has been investigated in the presence of lithium reference electrode. Fig. 19 shows the voltage variations of anode, cathode, and full cell made with MCMB anode during repeated overdischarges to −3.0 V. The cell was

discharged at 1 mA current drain. During first overdischarge, at around −0.9 V cell voltage, there is an indication of the onset of an electrochemical process. This electrochemical process took place at the anode as is evidenced from its voltage deflation at around 4.5 V corresponding to the cell voltage −0.9 V. The effect of overdischarge was more pronounced in the next two cycles and the cell failed to take charge after that. This is because, during overdischarge, copper dissolution occurs which ultimately transfers to cathode and causes cell shorting.

Fig. 20 represents the repeated overdischarge behavior of a lithium-ion cell made with C–C composite anode and LiCoO$_2$ cathode. The cell was overdischarged to −3.0 V at 1 mA current drain. There was no performance deterioration of C–C composite-based lithium-ion cell due to repeated
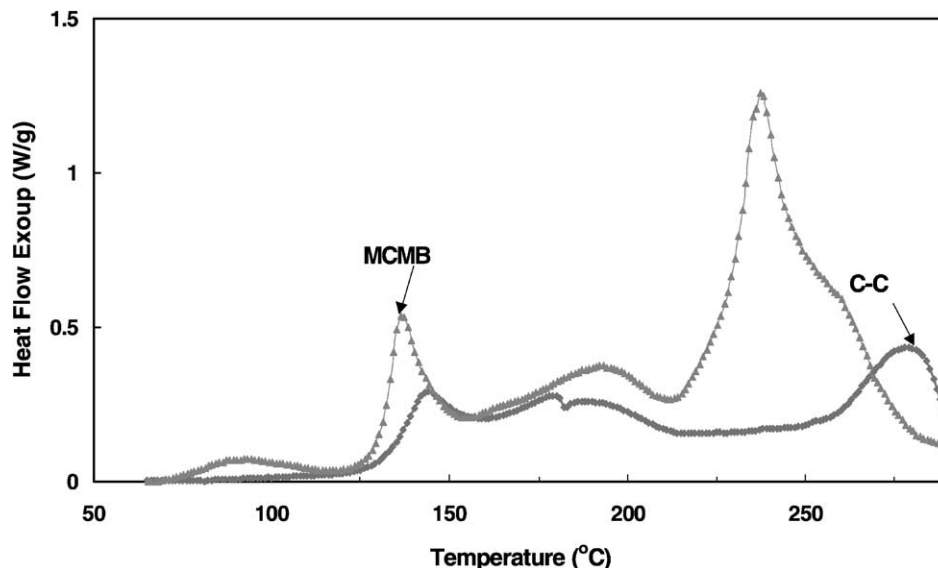

Fig. 21. Differential scanning calorimetry (DSC) results of fully charged MCMB 2528 and C–C composite anodes.

overdischarge. This is due to the absence of metallic substrate in C–C composite electrode.

3.7. Thermal stability

The thermal stability of fully charged C–C composite anode (lithiated C–C composite) was measured using DSC and is compared with that of fully charged MCMB carbon anode in Fig. 21. The first peak is most probably associated with the breakdown of SEI layer and the second to the reaction of LiC_x-electrolyte [8–10]. As can be seen, the thermal stability of C–C composite is better than that of MCMB carbon. The better thermal stability of C–C composite over MCMB electrodes may be due to:

(i) the fact that chemical formula of lithiated C–C composite is LiC_x, where $x > 6$ due to the presence of excess active material;
(ii) very low surface area of C–C composite ($0.2 \ m^2/g$);
(iii) absence of binder and copper substrate in C–C composite; and
(iv) high thermal conductivity and fire retardant characteristics of C–C composite.

4. Conclusion

Mesocarbon microbead (MCMB 2528) from Osaka Gas and C–C composite made from pitch-based fiber have been investigated as anodes for lithium-ion batteries. C–C composite anode shows several advantages over MCMB anodes:

(i) The irreversible capacity loss of C–C composite is significantly lower than that of MCMB carbon.
(ii) The practical capacity of C–C composite anode (based on total anode weight) is almost equal to that of metallic lithium anode (based on total anode weight) and 50% higher than that of MCMB-based anode (based on total anode weight).
(iii) C–C composite anode based lithium-ion cells can accept repeated overdischarge without performance deterioration.
(iv) The extra capacity of C–C composite can be utilized to improve energy density and/or safety issues related to overcharge of lithium-ion cells.
(v) The thermal stability of fully charged C–C anode (lithiated anode) is much better than that of fully charged MCMB anode.

The C–C composite can, therefore, be considered as a very strong candidate for the anodes of next generation relatively safe high energy density lithium-ion batteries.

References

[1] K. Sato, M. Noguchi, A. Demachi, N. Oki, M. Endo, Science 264 (1994) 556.
[2] M. Endo, C. Kim, K. Nishimura, T. Fujino, K. Miyashita, Carbon 38 (2000) 183–197.
[3] M. Dubois, A. Naji, J.P. Buisson, B. Humbert, E. Grivei, D. Billaud, Carbon 38 (2000) 1411–1417.
[4] A. Mabuchi, K. Tokumttsu, H. Fujimoto, T. Kasuh, in: Proceedings of the 7th International Meeting on Lithium Batteries, Extended Abstracts, Boston, MA, 15–20 May 1994, p. 212.
[5] S. Hossain, Y. Saleh, R. Loutfy, J. Power Sources 96 (2001) 5–13.
[6] S. Hossain, Y. Saleh, R. Loutfy, in: Proceedings of the 18th International Seminar & Exhibit on Primary & Secondary Batteries, Fort Lauderdale, FL, 5–8 March 2001.
[7] S. Hossain, Y. Kim, Y. Saleh, R. Loutfy, in: Proceedings of the 17th Annual Battery Conference, Long Beach, CA, 15–18 January 2002.
[8] A. DuPasquier, F. Disma, T. Bowmer, A.S. Gozdz, G. Amatucci, J.-M. Tarascon, J. Electrochem. Soc. 145 (1998) 472–477.
[9] Z. Zhang, D. Fouchard, J.R. Rea, J. Power Sources 70 (1998) 16–20.
[10] M.N. Richard, J.R. Dahn, J. Electrochem. Soc. 146 (1999) 2069.